Supplementary material

Effect of Sand Co-Presence on Cr^{VI} Removal in Fe^0-H_2O System

Marius Gheju, Ionel Balcu

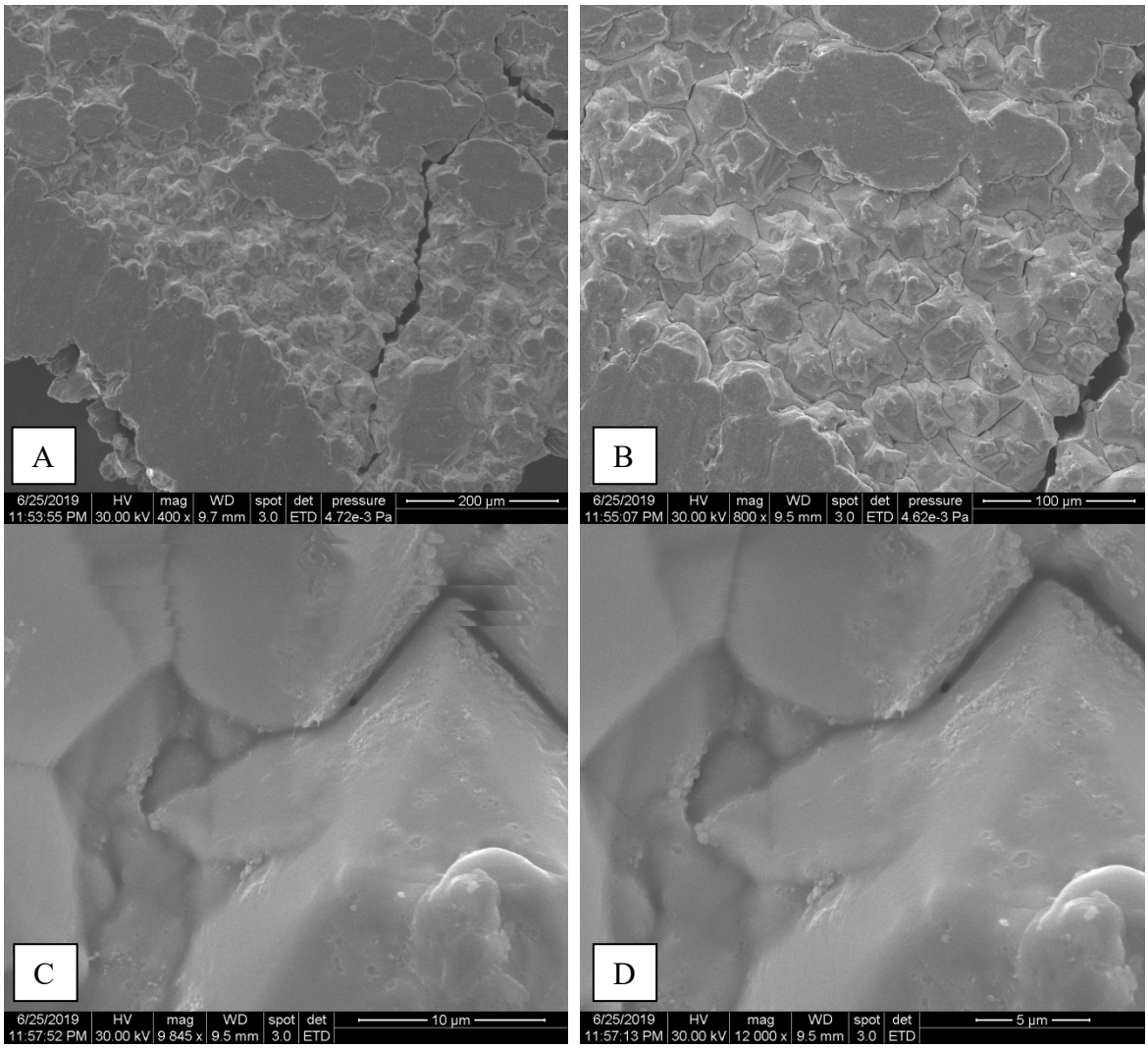

Figure S1. SEM micrograph of fresh Fe^0 at different magnifications

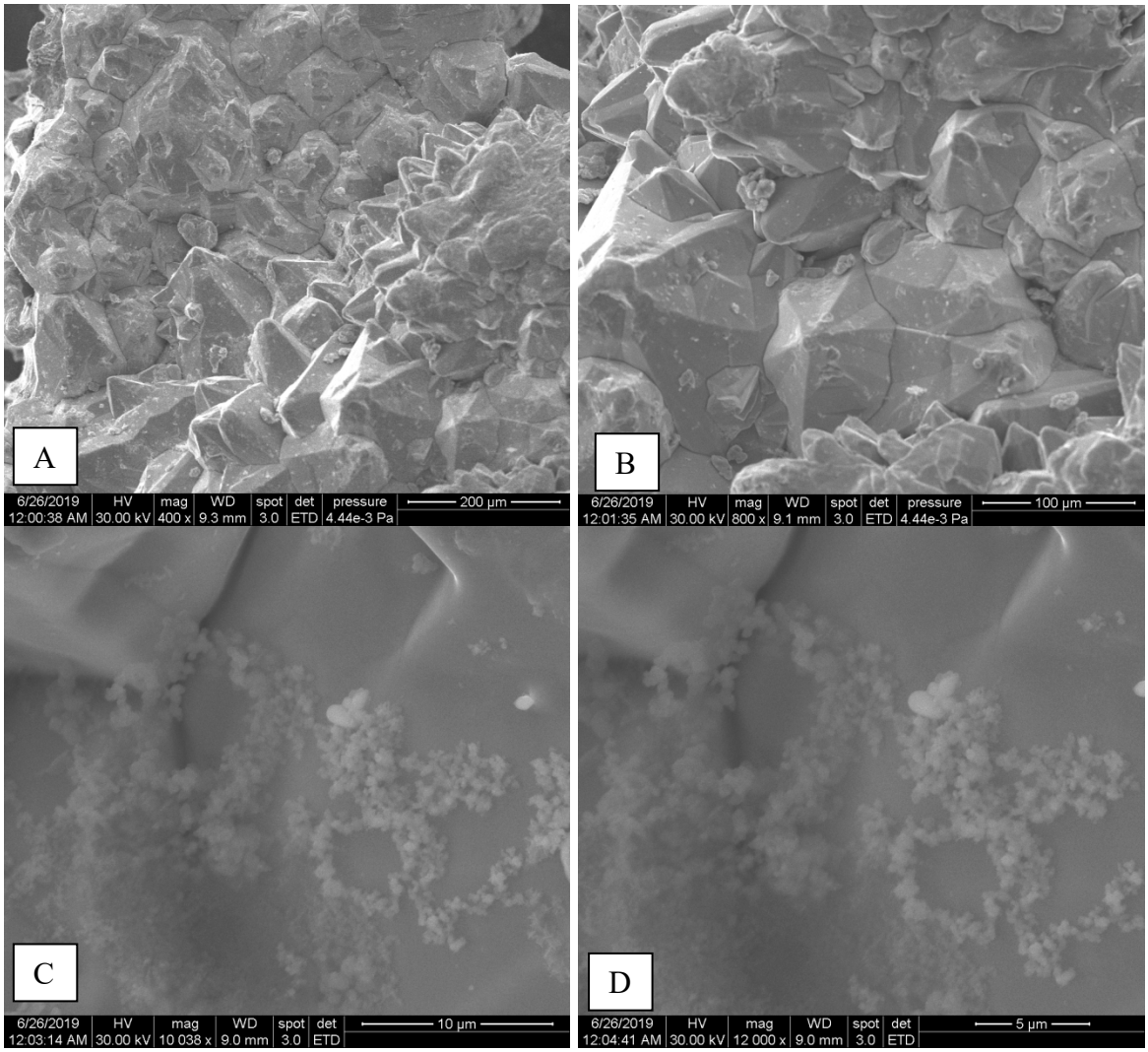

Figure S2. SEM micrograph of exhausted Fe^0 from 100% Fe^0 system at different magnifications

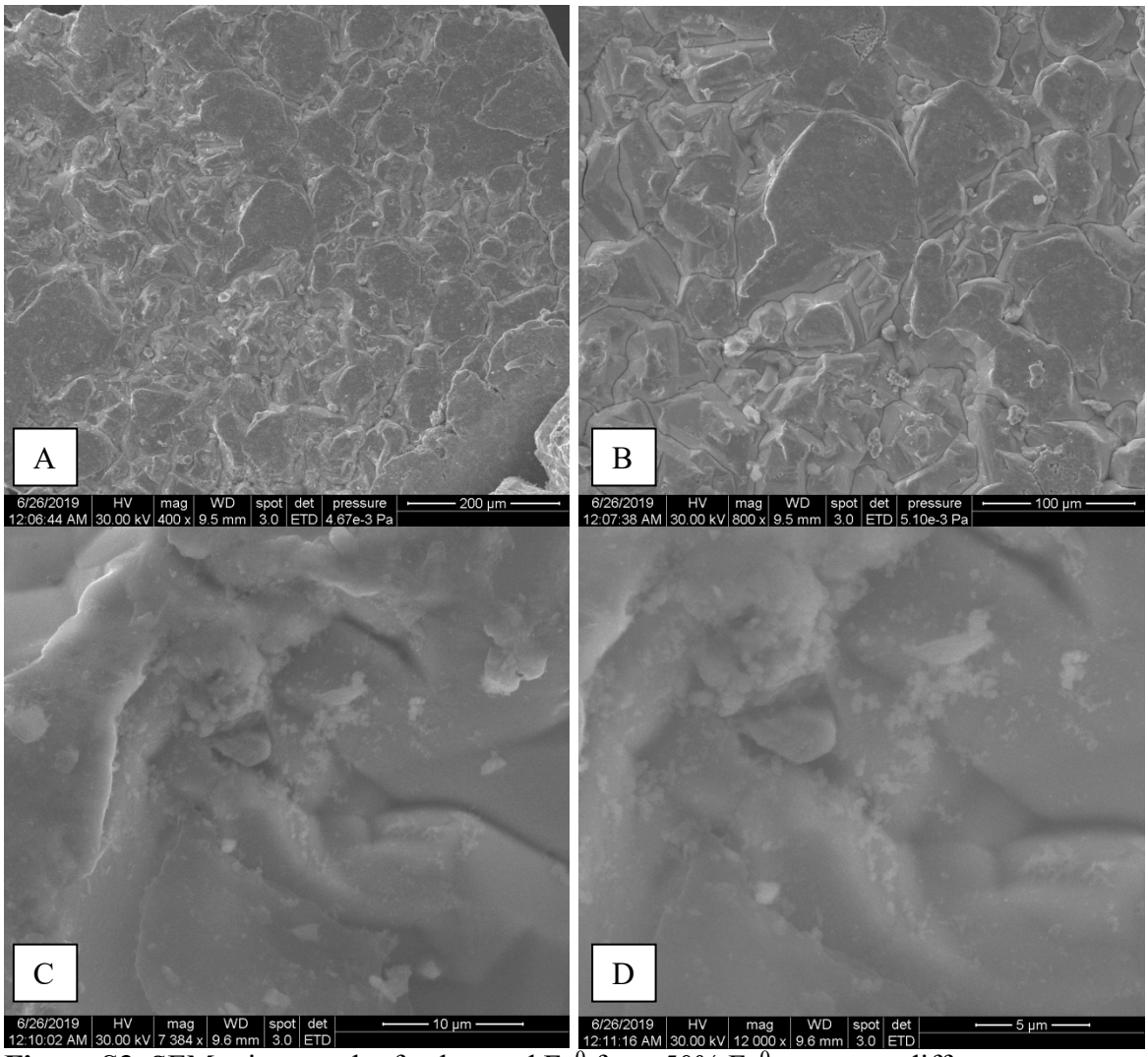

Figure S3. SEM micrograph of exhausted Fe^0 from 50% Fe^0 system at different magnifications

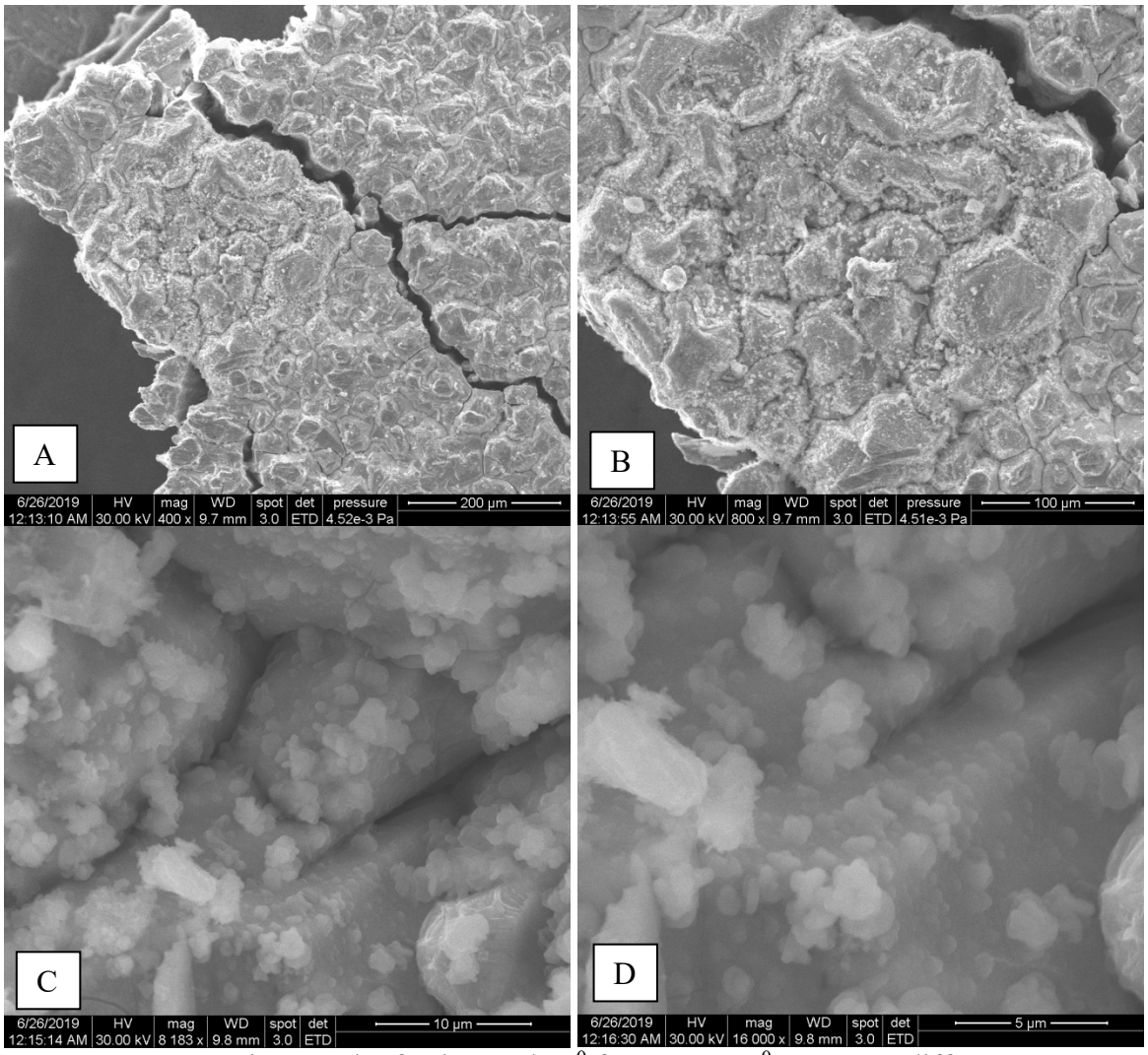

Figure S4. SEM micrograph of exhausted Fe^0 from 20% Fe^0 system at different magnifications

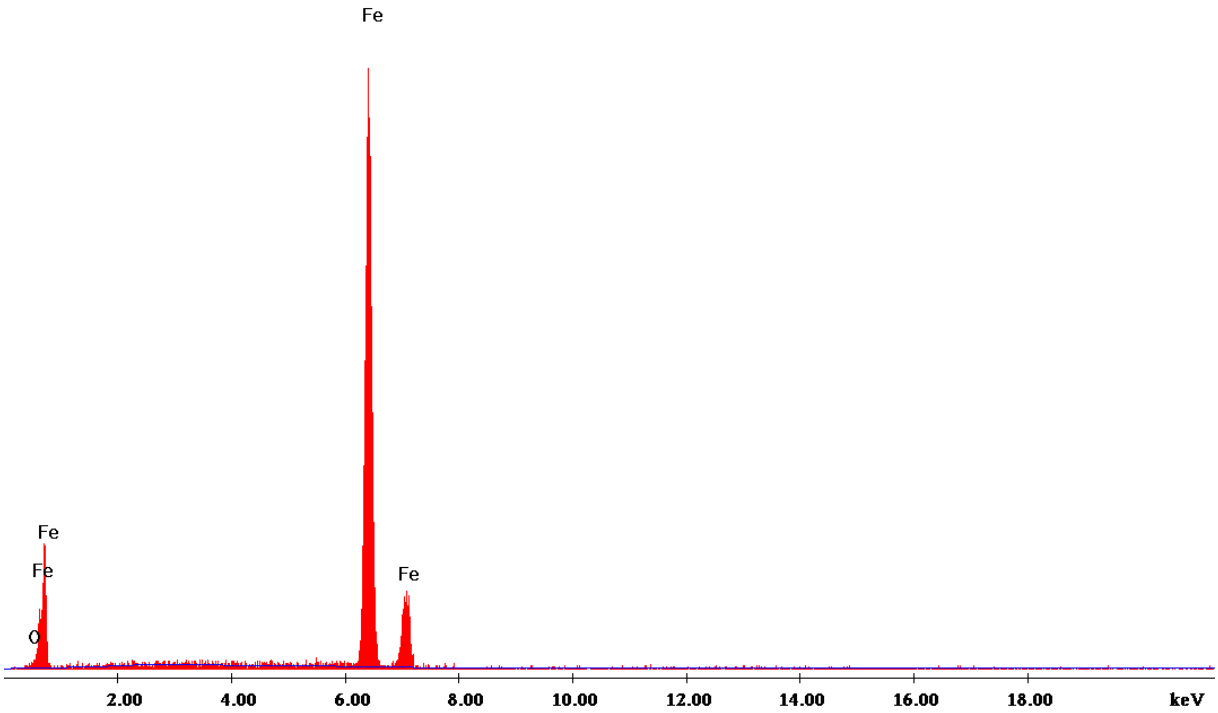

Figure S5. EDX pattern of fresh Fe^0

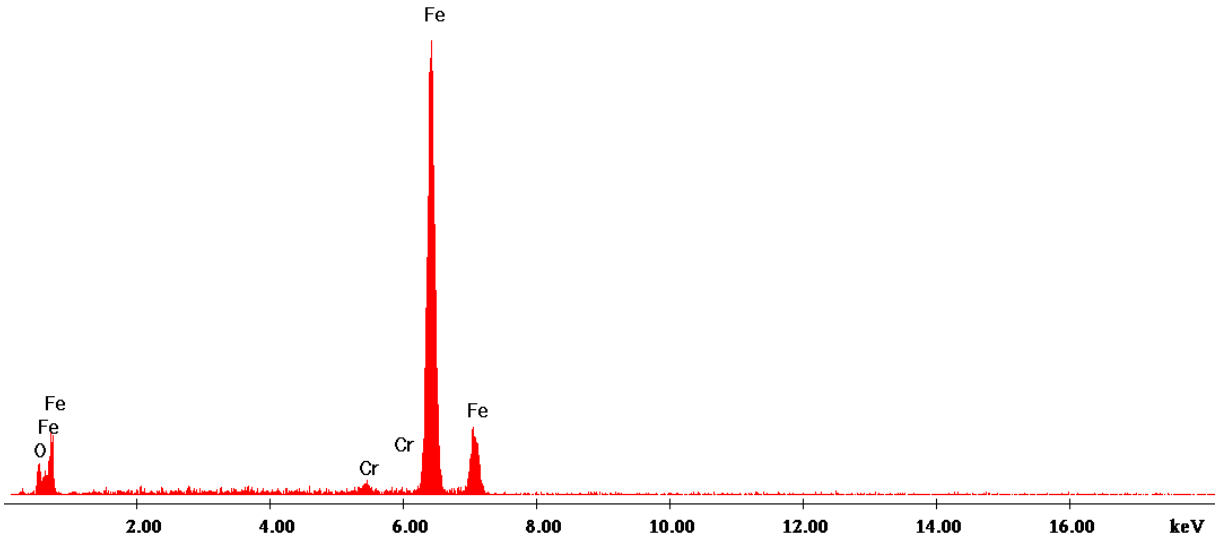

Figure S6. EDX pattern of exhausted Fe^0 from "Fe^0 only" system

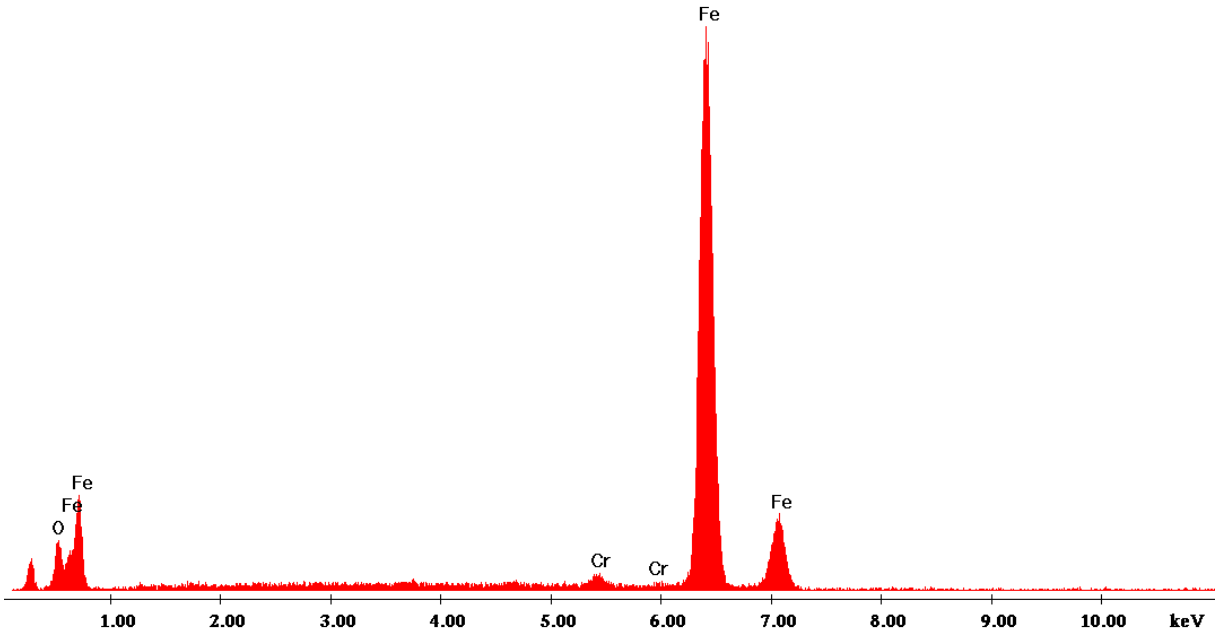

Figure S7. EDX pattern of exhausted Fe^0 from "50% Fe^0 + 50% sand" system

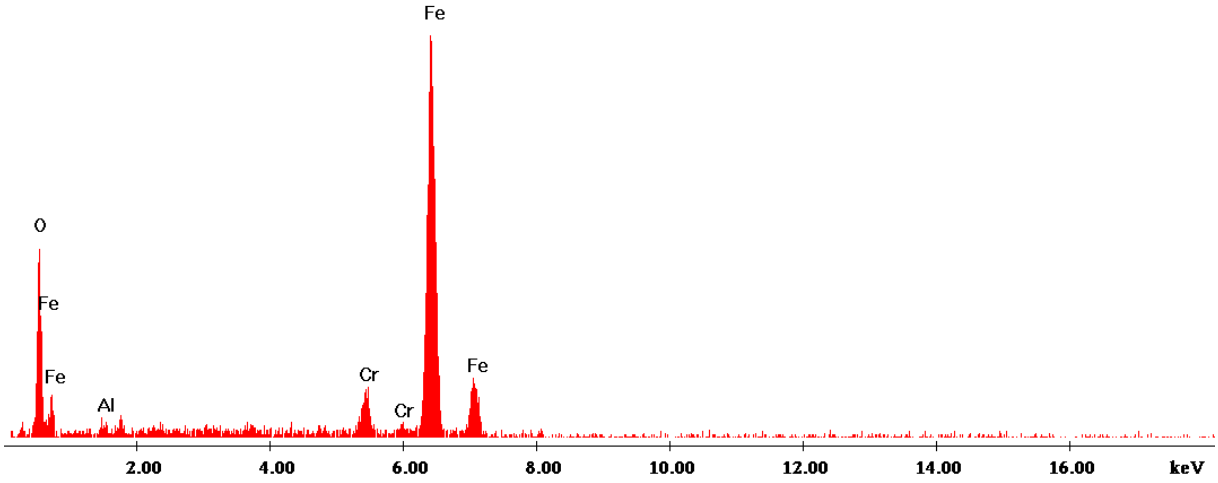

Figure S8. EDX pattern of exhausted Fe^0 from "20% Fe^0 + 80% sand" system

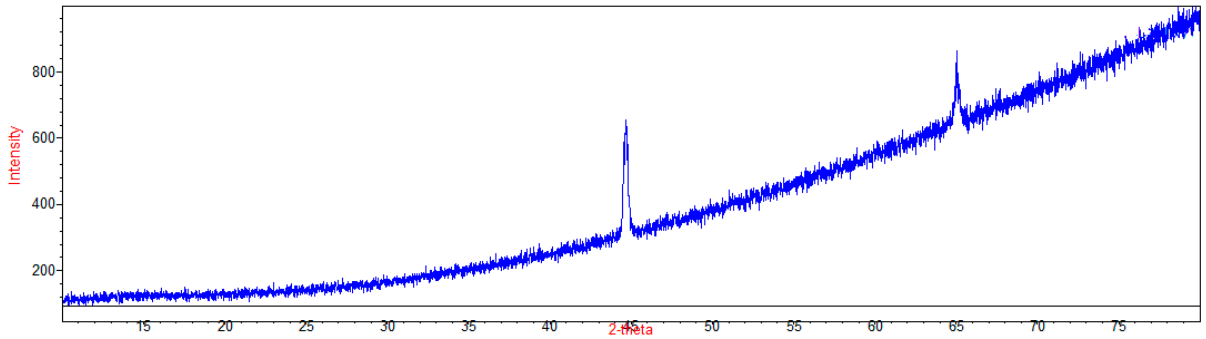

Figure S9. XRD pattern of fresh Fe^0

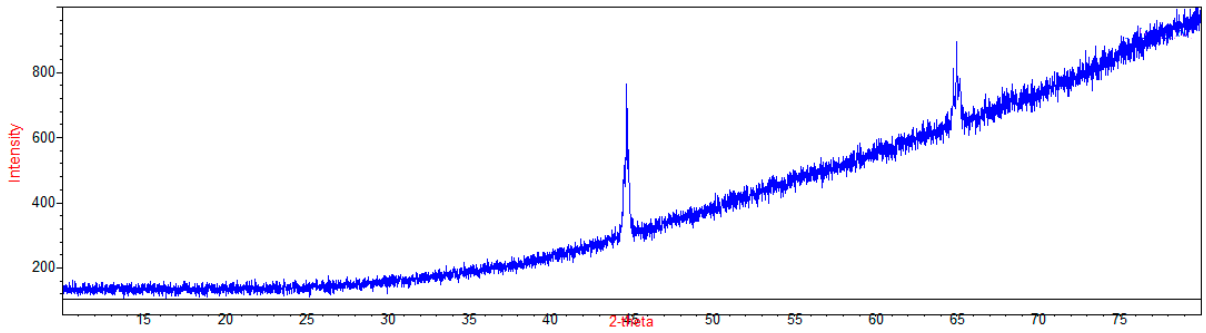

Figure S10. XRD pattern of exhausted Fe^0 from 100% Fe^0 system

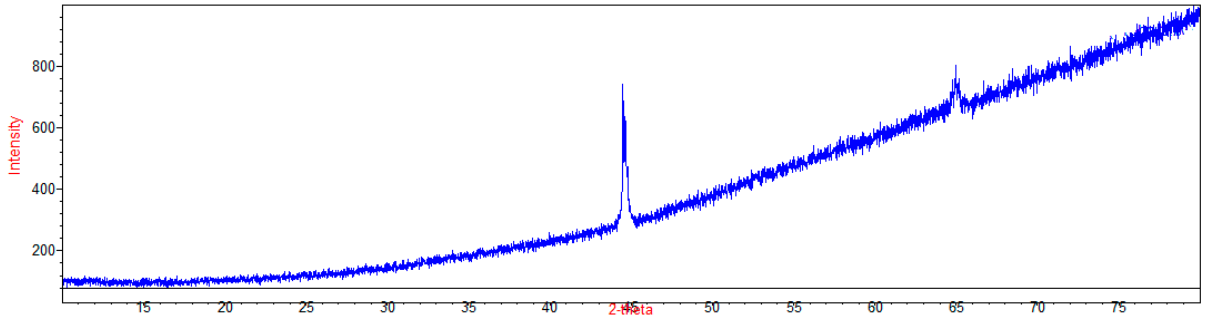

Figure S11. XRD pattern of exhausted Fe^0 from 50% Fe^0 system

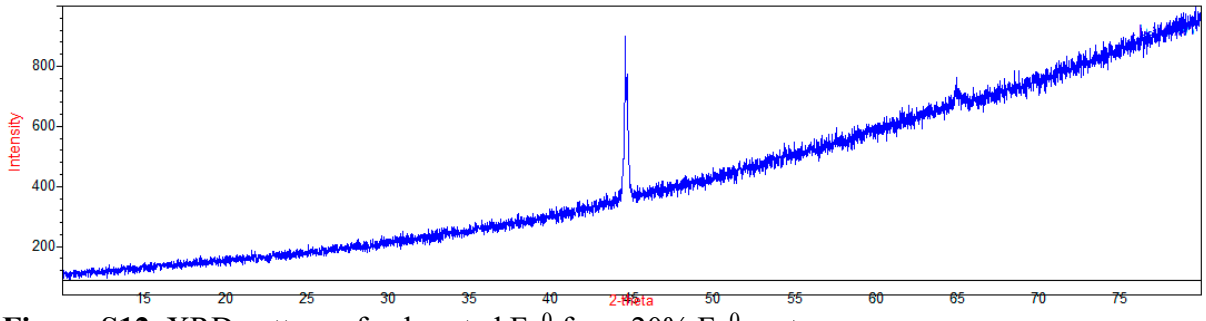

Figure S12. XRD pattern of exhausted Fe^0 from 20% Fe^0 system

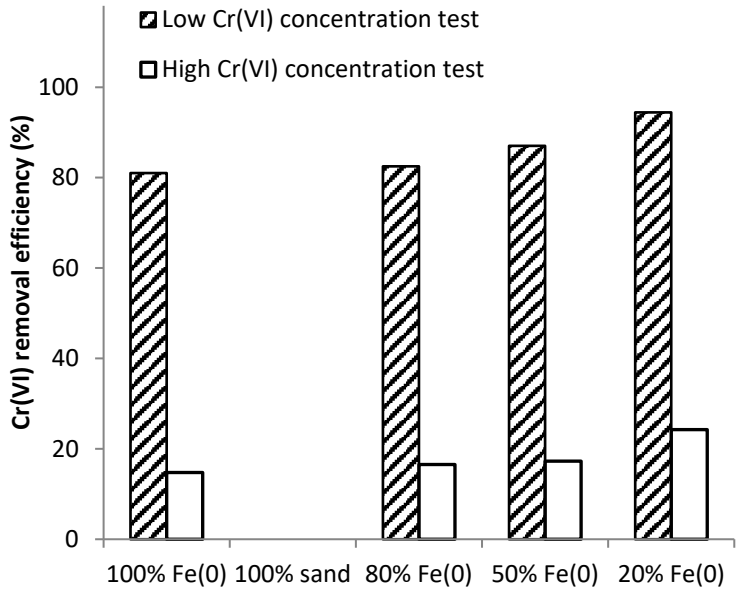

Figure S13. Profiles of Cr^{VI} removal efficiencies for non-disturbed batch experiments, after 40 experimental days.

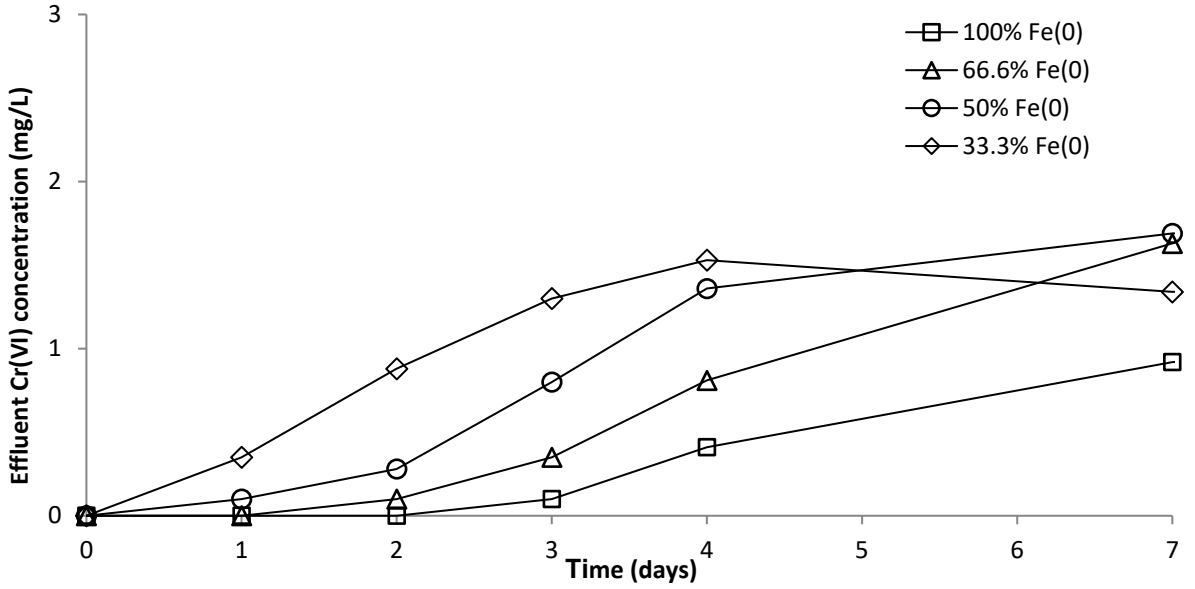

Figure S14. Evolution of Cr^{VI} breakthrough at pH 6.5, for columns having fixed Fe^0 volume and variable total reactive zone volume V_2.

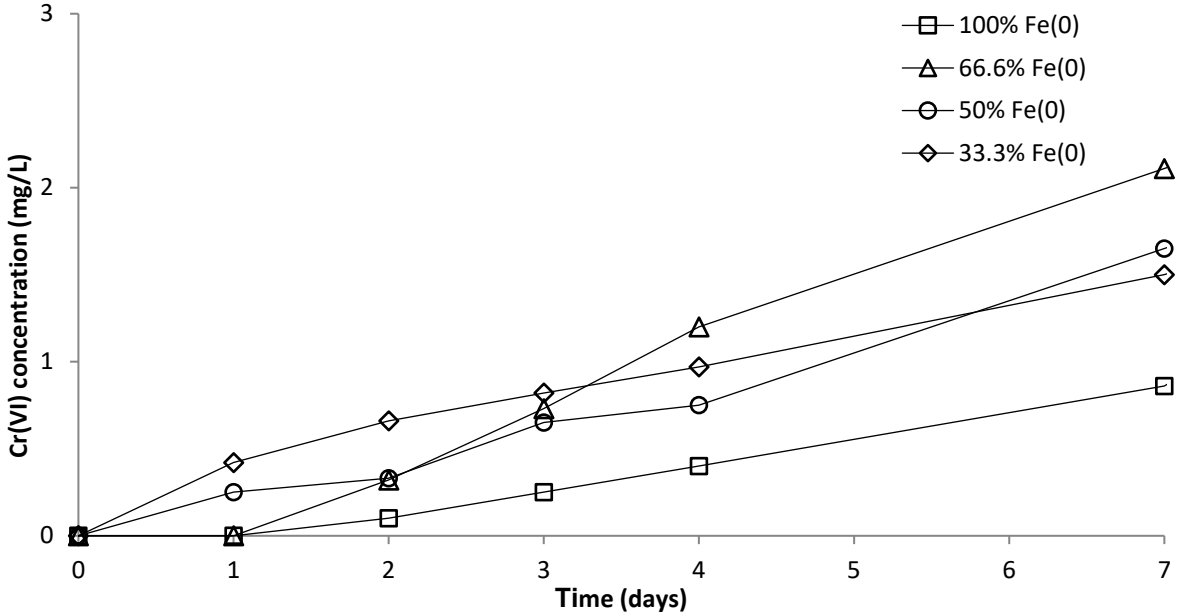

Figure S15. Evolution of Cr^{VI} breakthrough at pH 7.1, for columns having fixed Fe^0 volume and variable total reactive zone volume V_2.

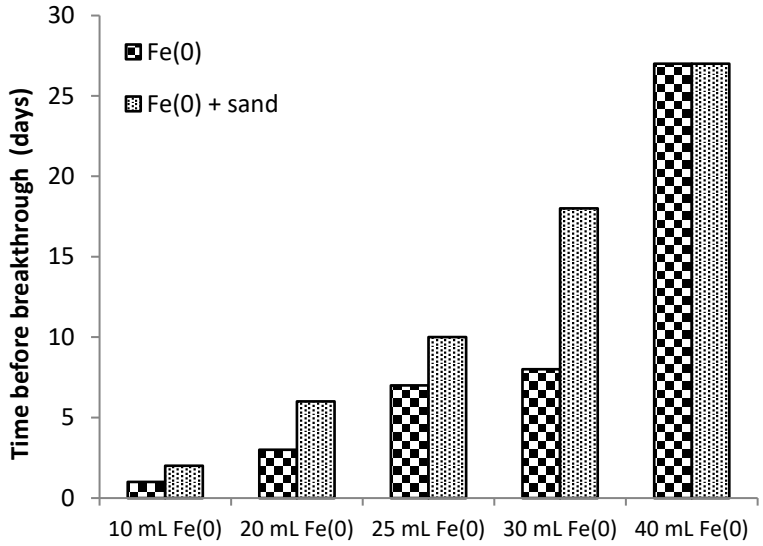

Figure S16. Evolution of Cr^{VI} breakthrough, for columns having variable Fe^0 volume and fixed total reactive zone volume V_2.